Quantum Electronics **49** (5) 455–463 (2019)

https://doi.org/10.1070/QEL17003

Effect of dipole blockade on the laser excitation spectra of mesoscopic ensembles of cold Rydberg atoms

I.I. Ryabtsev, I.I. Beterov, D.B. Tretyakov, E.A. Yakshina, V.M. Entin

Abstract. **The results of theoretical calculations of the multiatom laser excitation spectra of Rydberg atoms under conditions of a dipole blockade are presented, and the effect of the laser radiation line width and the interaction energy of Rydberg atoms on the dipole blockade completeness degree is discussed. It is shown that in order to increase the fidelity of performing quantum gates based on a dipole blockade, it is necessary to use resonance dipole–dipole interaction and exciting laser radiation with a line width smaller than 10 kHz.**

Keywords: *Rydberg atoms, laser excitation, dipole blockade.*

1. Introduction

Atoms in highly excited (Rydberg) states with principal quantum number $n \gg 1$ interact with each other much stronger than atoms in the ground state, because the energy of the resonant dipole–dipole interaction grows like n^4, and the van der Waals interaction like n^{11} [1]. This property of Rydberg atoms is used to obtain quantum entangled states and realise two-qubit and multi-qubit gates based on single neutral alkali metal atoms in arrays of optical dipole traps [2, 3].

With the use of Rydberg atoms, entangled states can be obtained in various ways. In the first theoretical work on this topic [4], it was proposed to use the interaction of the dipole moments of Rydberg atoms induced using a dc electric field. This interaction causes a change in the phase of the collective wave function. However, since the interaction energy of Rydberg atoms strongly depends on the distance between them, such a scheme turns out to be sensitive to the accuracy of the spatial localisation of atoms in traps. Therefore, in our papers [5–7], it was proposed to use the adiabatic passage of Förster resonances in the interaction of Rydberg atoms to reduce the dependence on the interatomic distance.

I.I. Ryabtsev, D.B. Tretyakov, E.A. Yakshina, V.M. Entin Rzhanov Institute of Semiconductor Physics, Siberian Branch, Russian Academy of Sciences, prosp. Akad. Lavrent'eva 13, 630090 Novosibirsk, Russia; Novosibirsk State University, ul. Pirogova 2, 630090 Novosibirsk, Russia; e-mail: ryabtsev@isp.nsc.ru;
I.I. Beterov Rzhanov Institute of Semiconductor Physics, Siberian Branch, Russian Academy of Sciences, prosp. Akad. Lavrent'eva 13, 630090 Novosibirsk, Russia; Novosibirsk State University, ul. Pirogova 2, 630090 Novosibirsk, Russia; Novosibirsk State Technical University, prosp. K. Marksa 20, 630073 Novosibirsk, Russia

Received 12 March 2019
Kvantovaya Elektronika **49** (5) 455–463 (2019)
Translated by V.L. Derbov

Another option was considered in Ref. [8], in which it was proposed to use a change in the spectrum of collective excitation of an ensemble of interacting Rydberg atoms (the effect of 'dipole blockade'). Its essence consists in the fact that in the presence of interaction, the excitation of one Rydberg atom in a small volume shifts the frequencies of resonances and blocks the excitation of other atoms. Therefore, only one Rydberg atom from the entire mesoscopic ensemble can be excited. This effect is insensitive to small variations in interatomic distances, and so quantum gates based on it can be performed with high accuracy. Obtaining entangled states and implementing the CNOT gate based on dipole blockade for two atoms located in two optical dipole traps separated by 5–10 μm were first demonstrated by M. Saffman's group from the USA [9] and A. Browaeys' group from France [10]. Experimental and theoretical studies of the dipole blockade were considered in reviews [2, 11, 12].

In most of the experiments mentioned, only the time dependences of the populations of the Rydberg states were presented and the changes in the laser excitation spectra under complete or partial dipole blockade were not discussed. These changes may carry additional information about the degree of blockade and the influence of various factors on it. In particular, the degree of the blockade completeness is determined by the ratio between the interaction energy of Rydberg atoms and the spectral width of the laser excitation, which is determined mainly by the Rabi frequency and the width of the laser line, therefore, the spectra can strongly depend on this width.

In our recent experimental work on three-photon laser excitation of $5S_{1/2} \rightarrow 5P_{3/2} \rightarrow 6S_{1/2} \rightarrow 37P_{3/2}$ of the Rydberg state $37P_{3/2}$ in Rb atoms, the dependence of the shape of the three-photon excitation spectrum on the number of atoms detected by selective field ionisation was studied [13]. Using the original technique, post-selection of signals was performed according to the number of registered atoms, $N = 1–5$. In the absence of a dipole blockade, it was found that with an increase in the average number of atoms in the centre of the spectrum of single-atom excitation ($N = 1$), a dip is observed, due to the features of the statistics of excitation and registration of Rydberg atoms. However, with a complete dipole blockade, only one atom can be excited to the Rydberg state from the entire mesoscopic ensemble. Therefore the dipole blockade should lead to a radical change in the multiatom spectra, namely, the dip in the single-atom spectrum ($N = 1$) should turn into a peak, and all other multiatom resonances should disappear. If they do not disappear completely, this may indicate an incomplete dipole blockade, and a change in the ratio of the amplitudes of multiatom resonances should make it possible to determine the degree of the dipole

blockade completeness under specific experimental conditions.

This paper presents the results of theoretical calculations of the spectra of multiatom laser excitation under conditions of a dipole blockade and discusses the influence of the laser radiation line width and the interaction energy of Rydberg atoms on the degree of the dipole blockade completeness.

2. Theoretical model of a dipole blockade in an ensemble of two atoms

First, consider the theoretical model of the dipole blockade using the example of two atoms. They can either be spatially localised in separate optical dipole traps with the distance R between them being of a few micrometers, or be in a single volume of laser excitation and have a random position in it [14]. Optical dipole traps are produced by tight focusing of nonresonant laser radiation, which in the case of being detuned to the red from resonance provides the capture and trapping of atoms in the region of the maximum intensity of the laser field due to the gradient dipole force [2]. With a small radius of the beam waist ($\sim$1 μm) in such traps, a collisional blockade takes place and it is possible to trap exactly one atom in the trap, and the effect of dipole blockade is usually observed for two atoms in adjacent traps with a distance of 5–10 μm between them. A single volume can be formed at the intersection of focused laser beams that excite Rydberg states, as in our experiments [13, 15, 16]. In this work, we confine ourselves to the analysis of the effect of the dipole blockade in a single excitation volume corresponding to our experimental conditions.

The interaction of atoms in the Rydberg states is most conveniently considered under the conditions of Förster resonances, which we studied in earlier papers [5–7, 14–16]. Such resonances occur, e.g., when the Rydberg level 2, excited by laser radiation from the ground state 0, lies in the middle between two adjacent levels 1 and 3 of opposite parity (Fig. 1a). An example is the Förster resonances $n\mathrm{P}_{3/2} + n\mathrm{P}_{3/2} \rightarrow n\mathrm{S}_{1/2} + (n+1)\mathrm{S}_{1/2}$ in Rydberg Rb atoms [15]. In the absence of electric field, they have small energy defects $\Delta = W(n\mathrm{S}_{1/2}) + W((n+1)\mathrm{S}_{1/2}) - 2W(n\mathrm{P}_{3/2})$ which depend on n. Here $W(nL_J)$ is the energy of Rydberg states in units of frequency. For $n \leqslant 38$, the energy defect can be made equal to zero due to the Stark effect in a dc electric field, and for states with greater n, a combination of dc and radio frequency fields is required [15, 16]. At $\Delta = 0$, a resonant dipole–dipole interaction with the energy proportional to R^{-3} arises between the atoms, and for larger Δ there is a weaker van der Waals interaction with the energy proportional to R^{-6}. Thus, using the electric field and Förster resonances, one can substantially change the character of the interaction of Rydberg atoms.

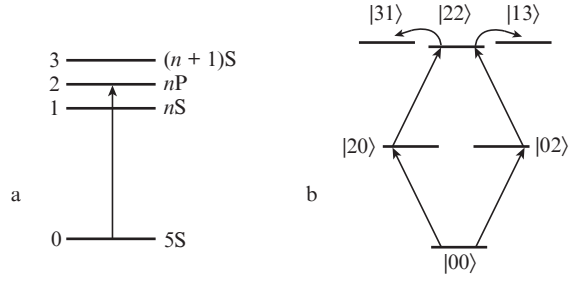

Figure 1. (a) Scheme of laser excitation of a single Rydberg atom of Rb(nP) and the states involved in the Förster resonance $n\mathrm{P}_{3/2} + n\mathrm{P}_{3/2} \rightarrow n\mathrm{S}_{1/2} + (n+1)\mathrm{S}_{1/2}$, as well as (b) the scheme of transitions between the collective states of two atoms.

To study the effect of the dipole blockade upon laser excitation of interacting Rydberg atoms, it is necessary to consider transitions between different collective states of two atoms (Fig. 1b). The resonant laser radiation causes transitions between the states $|00\rangle \rightarrow |02\rangle$, $|20\rangle \rightarrow |22\rangle$, and the state $|22\rangle$ is coupled by the operator of dipole–dipole interaction with the states $|31\rangle$, $|13\rangle$, which causes the transitions $|22\rangle \rightarrow |31\rangle, |13\rangle$. As a result of the interaction, the state $|22\rangle$ shifts in energy, which leads to the effect of a dipole blockade. The parameters of this problem are the Rabi frequency Ω and the frequency detuning δ at the optical transition $0 \rightarrow 2$ in a separate atom, the matrix element of the resonant dipole–dipole interaction operator V on the transitions $|22\rangle \rightarrow |31\rangle, |13\rangle$, and the defect Δ of the Förster resonance.

For two Rydberg atoms in the initial state $n\mathrm{P}_{3/2}(|M| = 1/2)$, the matrix element of the dipole–dipole interaction operator is given by the expression

$$V = \frac{d_1 d_2}{4\pi\varepsilon_0}\left(\frac{1}{R^3} - \frac{3Z^2}{R^5}\right), \tag{1}$$

where d_1 and d_2 are the z-components of the dipole moment matrix elements of the transitions $|n\mathrm{P}_{3/2}(|M| = 1/2)\rangle \rightarrow |n\mathrm{S}_{1/2}(|M| = 1/2)\rangle$ and $|n\mathrm{P}_{3/2}(|M| = 1/2)\rangle \rightarrow |(n+1)\mathrm{S}_{1/2}(|M| = 1/2)\rangle$, respectively; Z is the z-component of the vector $\boldsymbol{R}$ connecting two atoms (the z axis is chosen along the direction of the control electric field); and ε_0 is the dielectric constant. Here, for simplicity, we consider only transitions without changing the projection of the moment M, because otherwise, it is necessary to take into account the structure of magnetic sublevels, which will complicate the task dramatically. As discussed in our paper [16], the energy shift δW_{22} of the collective state $|22\rangle$ in the case of the Förster resonance is described by the approximate expression:

$$\delta W_{22} = \pm\left(\sqrt{\frac{\Delta^2}{4} + 2V^2} - \frac{|\Delta|}{2}\right). \tag{2}$$

Here, the sign is taken positive if the state $|22\rangle$ lies above the states $|31\rangle$, $|13\rangle$, and vice versa. At $\Delta = 0$, the interaction is a resonance dipole–dipole one, and the state $|22\rangle$ splits into two sublevels with energies $\pm\sqrt{2}V = C_3/R^3$, and for large Δ, it becomes a van der Waals one with an energy of $\pm 2V^2/\Delta = C_6/R^6$, where C_3 and C_6 are interaction constants [17].

To calculate the laser excitation spectra with the dipole blockade, it is necessary to solve the time evolution problem in the six-level system shown in Fig. 1b, with the initial condition of both atoms being in the ground state 0. This can be done most simply by solving the nonstationary Schrödinger equation [14]. However, this approach does not take into account the finiteness of the Rydberg atom lifetime [18], and it is also difficult to take into account the finite width of the laser radiation line Γ. Both of these factors lead to parasitic broadening and loss of coherence, which can affect the completeness of the dipole blockade. Therefore, it would be preferable to solve the problem using the density matrix technique, which allows introducing the terms responsible for relaxation and dissipative processes, in the same way as in our earlier analysis of the three-photon laser excitation spectra and Förster resonances in Rydberg atoms [15, 19].

Nevertheless, the application of the Schrödinger equation can be adequate to the task if we consider the excitation of atoms by short laser pulses (1–2 μs) to high Rydberg states with $n \geqslant 100$ that have lifetimes on the order of hundreds of microseconds or longer [18]. Moreover, since for such short pulses the laser radiation optical frequency, as a rule, does not experience noticeable fluctuations during the pulse, the finite width of the laser radiation line can be taken into account by averaging the obtained excitation spectra over the frequency fluctuations from pulse to pulse, assuming that in each individual laser pulse the radiation is monochromatic.

3. Spectra of a dipole blockade in an ensemble of two Rb atoms ($120P_{3/2}$)

As an example, we consider the effect of a dipole blockade for two Rb atoms excited in the high Rydberg state $120P_{3/2}$, which has a rather long lifetime (614 μs) at room temperature [18]. Figure 2a shows the numerically calculated Stark diagram of the Rydberg states of the Rb atom near the state $120P_{3/2}$. Since the polarisabilities of Rydberg states grow as n^7, the Stark effect manifests itself already at fields E of the order of several mV cm^{-1}, and at $E = 80$ mV cm^{-1}, the sets of hydrogen-like states with $n = 117$, 118 and large orbital angular momenta overlap. However, the S, P, and D states have large quantum defects and are subject to the quadratic Stark effect [20], with which one can control the position of energy levels and the Förster resonance.

When the Rydberg state $120P_{3/2}$ is excited for interacting atoms, the Förster resonance $120P_{3/2} + 120P_{3/2} \rightarrow 120S_{1/2} + 121S_{1/2}$ occurs, which in the absence of an electric field has a positive energy defect $\Delta = +60$ MHz (Fig. 2b). This resonance is 'inaccessible', since the application of a dc electric field only increases the energy defect and reduces the interaction energy in accordance with Eqn (2). However, in the presence of a dc field $E = 10$ mV cm^{-1} and a radio frequency field $E \approx 1$ mV cm^{-1} with a frequency of 76.67 MHz, the energy defect can be fully compensated. As we have shown in Ref. [16], the radio-frequency field efficiently produces additional collective Floquet Rydberg levels, which then undergo intersections and are equivalent to the exact Förster resonance. Therefore, below we consider two cases with different energy defects: $\Delta = +60$ MHz in the absence of an electric field and $\Delta = 0$ in the presence of dc and radio-frequency electric fields.

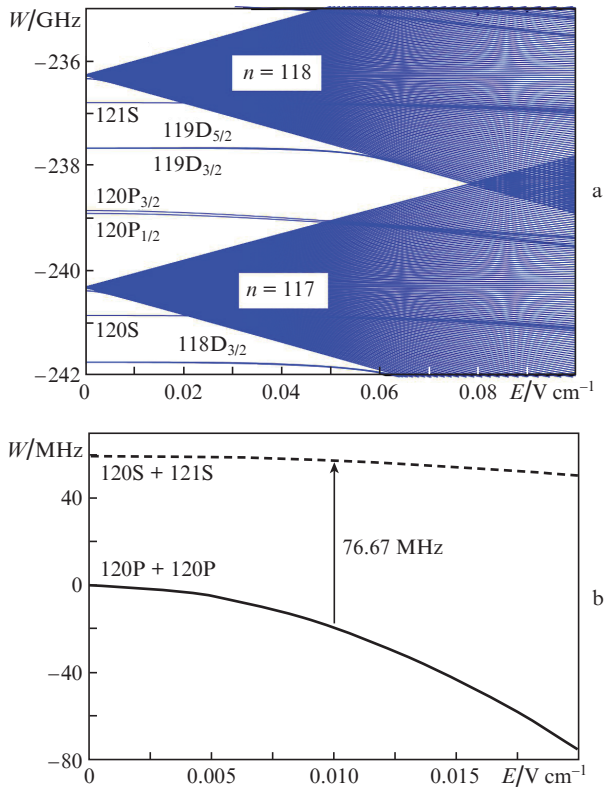

Figure 2. Dependences of the energies of collective two-body states W on the electric field E: (a) the Stark diagram of the Rydberg states of the Rb atom near the state 120P and (b) the Förster resonance $120P_{3/2} + 120P_{3/2} \rightarrow 120S_{1/2} + 121S_{1/2}$ in Rydberg Rb atoms.

The calculated values of the radial parts of the transition dipole moments for this Förster resonance are about 15000 a.u.; therefore, the atoms in the Rydberg state $120P_{3/2}$ interact strongly at distances of 10–20 μm. For example, the matrix element of the dipole–dipole interaction operator V amounts to ~15 MHz for $R = 15$ μm, ~50 MHz for $R = 10$ μm and ~400 MHz for $R = 5$ μm. When these values are substituted into Eqn (2) for $\Delta = +60$ MHz, it can be found that at $R = 15$ μm there is a relatively weak van der Waals interaction, and at $R = 5$ μm, the detuning Δ becomes insignificant and an almost resonant dipole–dipole interaction is observed. With $\Delta = 0$ the interaction will be strong for all specified distances. Note that for two disordered atoms in a volume in the form of a cube with a side L, the average distance between the atoms R is approximately $L/2$ [14]. Although the shape of the real volume of excitation differs from the cubic one, the results of numerical calculations turn out to be insensitive to it and depend mainly on volume only.

Figure 3 presents the numerically calculated probability spectra of the single-atom (P_1) and two-atom (P_2) excitations of a high Rydberg state $120P_{3/2}$ with a rectangular laser pulse having the duration $\tau = 2$ μs for two Rb atoms in the cubic volume of the laser excitation. The spectra are averaged over 1000 random positions of two atoms. The linear size of the excitation volume L, the detuning from the Förster resonance Δ and the Rabi frequency Ω for the transition from the ground state to the Rydberg one are varied. The line width of the laser radiation is $\Gamma = 0$.

Figure 3a presents the probability spectra of the excitation of two noninteracting atoms ($V = 0$). The Rabi frequency is $\Omega = 0.25$ MHz. At $\tau = 2$ μs, this corresponds to a laser π-pulse, which transfers the entire population from the ground state to the Rydberg one. Since $\Gamma = 0$, full Rabi oscillations of the populations are present in the spectra. As we discussed in [13], in this case a dip is observed at the centre of the probability spectrum of single-atom excitation P_1 because both atoms pass into the Rydberg state and the probability P_2 is close to 1. As the Rabi frequency decreases to 0.177 MHz, the dip decreases noticeably (Fig. 3b), because the probability of excitation of the Rydberg state becomes smaller than 1.

Figure 3c shows the spectra of one- and two-atom excitations of interacting atoms at $L = 30$ μm, $\Omega = 0.25$ MHz, $\Delta = +60$ MHz. Since R in this case is nearly15 μm, the interaction is a weak van der Waals one, as discussed above. Therefore, the effect of dipole blockade only partially reduces P_2 (from 1 to 0.39) and increases P_1 (from 0 to 0.5) at the centres of resonances. As a result, the dip in the centre of the probability spectrum P_1 turns into a peak, which is the main signature of

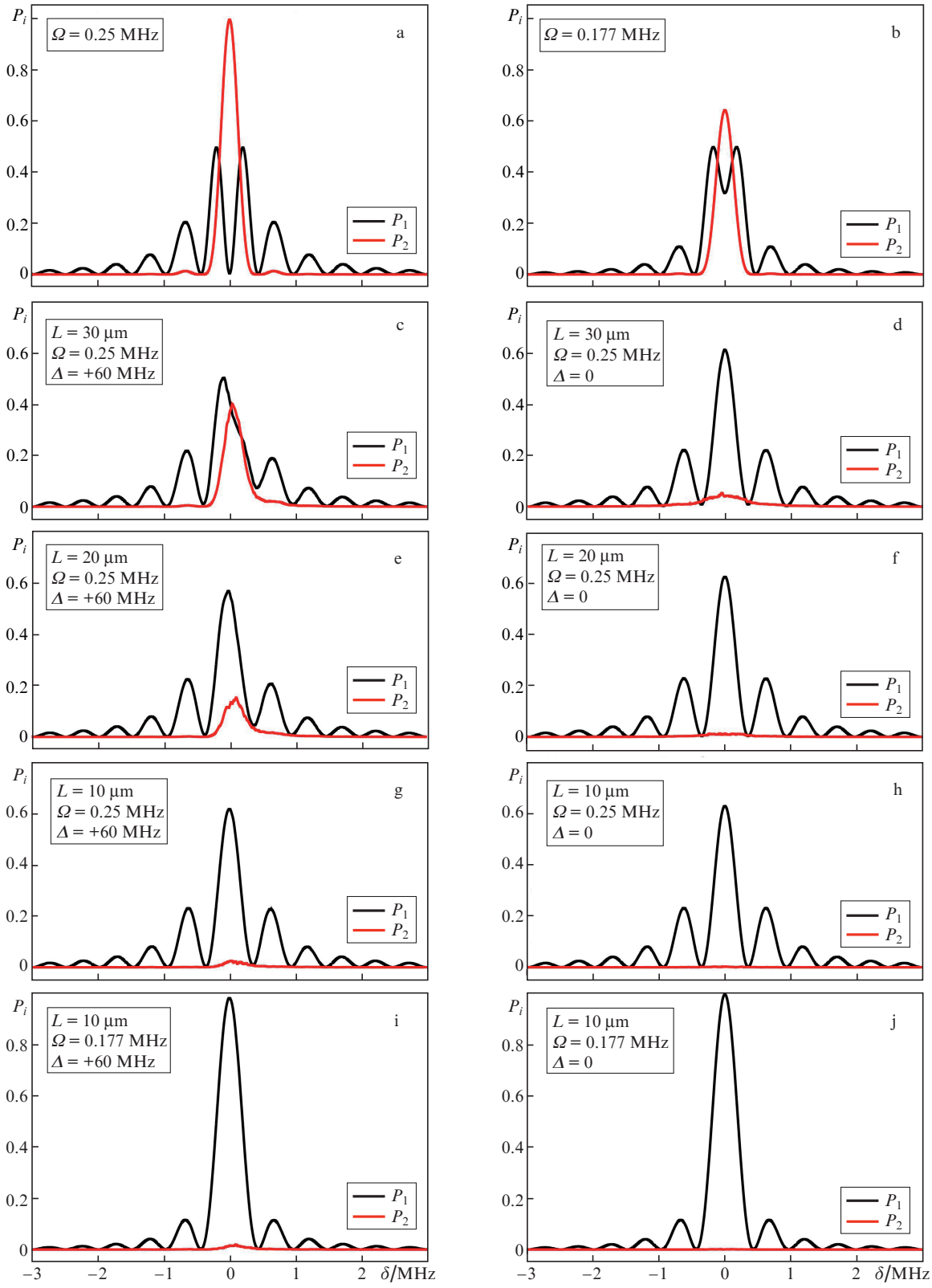

Figure 3. (Colour online) Calculated probability spectra of the single-atom (P_1) and two-atom (P_2) excitation of the Rydberg state $120P_{3/2}$ by a rectangular laser pulse having the duration 2 μs with different Rabi frequencies Ω for (a, b) two noninteracting and (c–j) interacting Rb atoms randomly positioned in the cubic volume of laser excitation with a linear size L, with various detunings from the Förster resonance Δ and the width of the laser line $\Gamma = 0$.

the presence of a dipole blockade. In addition, due to the van der Waals shift of the state $120P_{3/2}$, the centres of single-atom and two-atom excitations are shifted relative to each other by ~0.15 MHz, and the resonances themselves become asymmetric. This shift and asymmetry can also be indicative of a partial dipole blockade, since they are absent for noninteract-

ing atoms or in resonant dipole–dipole interaction. The case of $P_2 = 0$ corresponds to a complete dipole blockade; in this case P_1 must not necessarily be equal to 1. At $\Delta = 0$ (Fig. 3d), the energy of the resonant dipole–dipole interaction is sufficient for an almost complete dipole blockade. Even for such a large volume of excitation, the value of P_2 decreases from 1 to 0.045, and the value of P_1 increases from 0 to 0.62 (hereinafter, the probability values are given for $\delta = 0$).

A decrease in the linear size L of the excitation volume from 30 to 20 μm increases the average energy of the dipole–dipole interaction by a factor of 3.4. This leads to the fact that at $\Delta = +60$ MHz, the value of P_2 decreases to 0.15, and the value of P_1 increases to 0.56 (Fig. 3e), i.e., the efficiency of the dipole blockade increases significantly. At $\Delta = 0$ (Fig. 3e), for $L = 20$ μm, almost complete blockade is achieved: $P_2 = 0.007$ and $P_1 = 0.63$.

Further decrease in the size L to 10 μm increases the average energy of the dipole–dipole interaction by another 8 times. In this case, at $\Delta = +60$ MHz, the value of P_2 decreases further to 0.023, and the value of P_1 increases to 0.62 (Fig. 3g). At $\Delta = 0$ (Fig. 3h) for $L = 10$ μm, the complete blockade is achieved: $P_2 = 0.001$ and $P_1 = 0.63$. This means that the so-called radius of the dipole blockade [11] already significantly exceeds the size of the excitation volume, and regardless of the positions of two atoms in it, the effect of a complete dipole blockade will be observed.

For applications in quantum information, it is important that with a complete dipole blockade, the Rabi oscillations of populations remain, and they occur between the ground collective state $|00\rangle$ and the singly excited states $|02\rangle$, $|20\rangle$. However, from Fig. 3g we see that for a given Rabi frequency, the probability P_1 does not reach a maximum value of 1, and has saturation at a value of 0.62. This is due to the fact that the effective frequency of Rabi transitions to singly excited collective states increases by a factor of $\sqrt{2}$ with a complete dipole blockade, and in the general case for an ensemble of N atoms, it increases $\sqrt{N}$ times [11]. Therefore, in the case of two atoms, in order for P_1 to reach a value of 1, it is necessary to reduce Ω by a factor of $\sqrt{2}$.

Such spectra are presented in Figs 3i and 3j for $L = 10$ μm. Now with $\Delta = +60$ MHz, the value of P_2 is 0.021, and the value of P_1 increases to 0.989 (Fig. 3i). When $\Delta =$ (Fig. 3j), a complete blockade is achieved: $P_2 = 0.001$ and $P_1 = 0.999$. Since the dipole blockade directly generates quantum-entangled states of two atoms to perform quantum gates, Fig. 3j demonstrates the possibility of achieving the fidelity of quantum gates based on dipole blockade up to 99.9%. It is also seen from Fig. 3 that the presence of a nonzero energy defect for the Förster resonance under consideration reduces the fidelity of the dipole blockade by an order of magnitude. Therefore, despite the technical difficulty of using dc and radiofrequency electric fields in experiments with ultracold atoms, it is recommended to use only resonant dipole–dipole interaction of Rydberg atoms with a zero defect in the energy of the Förster resonance implemented with the electric field.

4. Dipole blockade spectra in an ensemble of three Rb atoms ($120P_{3/2}$)

An increase in the number of atoms in the mesoscopic ensemble significantly increases the number of collective basis states, which must be taken into account in the theoretical model of the dipole blockade at the Förster resonance. If for two atoms the calculations were performed with 6 basic states according to Fig. 1, then for three atoms it is necessary to solve the Schrödinger equation already with 20 basic states. Taking into account the necessity of averaging the dipole blockade spectra over the random positions of three atoms in the excitation volume, the numerical calculations take quite a long time. Therefore, in this paper, we restrict ourselves to calculations for only two and three atoms.

Figure 4a shows the probability spectra of the single-atom (P_1), two-atom (P_2), and three-atom (P_3) excitation of the Rydberg state $120P_{3/2}$ by a square laser pulse having the duration 2 μs for three noninteracting atoms ($V = 0$) at the Rabi frequency $\Omega = 0.25$ MHz corresponding to the laser π-pulse. The width of the laser line is $\Gamma = 0$; therefore, the full Rabi oscillations of the populations are present in the spectra. As in the case of two atoms, in the centre of the probability spectra P_1 and P_2 there are dips because all three atoms pass into the Rydberg state and the probability P_3 is close to 1. When the Rabi frequency decreases to 0.144 MHz (by $\sqrt{3}$ times), corresponding to the maximum of single-atom excitation with a full dipole blockade, the dips noticeably decrease, since the probability of the Rydberg state excitation becomes less than 1 (Fig. 4b).

Figure 4c presents the probability spectra P_1, P_2, and P_3 for interacting atoms at $L = 30$ μm, $\Omega = 0.25$ MHz, and $\Delta = +60$ MHz. As discussed above, under these conditions the interaction is a weak van der Waals one. Therefore, at the centres of resonances, the effect of dipole blockade greatly reduces P_3 (from 1 to 0.07), but also increases P_2 (from 0 to 0.38) and P_1 (from 0 to 0.27), and the dip in the centre of the spectrum of the probability P_2 turns into a peak. As in the case of two atoms, it turns out that because of the van der Waals shift of the state $120P_{3/2}$, the resonance centres are shifted relative to each other by ~0.15 MHz, and the resonances themselves are asymmetric. At $\Delta = 0$ (Fig. 4,d), the energy of the resonant dipole–dipole interaction is sufficient for an almost complete dipole blockade: P_3 decreases from 1 to 0.001, although P_2 increases from 0 to 0.07, and P_1 increases from 0 to 0.19.

The reduction of the size L from 30 to 20 μm (Fig. 4e) leads to the fact that at $\Delta = +60$ MHz the value of P_3 decreases to 0.0008, P_2 decreases to 0.2, and P_1 does not change. At $\Delta = 0$ (Fig. 4f) for $L = 20$ μm, almost complete blockade is achieved: P_3 decreases to 0.0001, P_2 decreases to 0.02, and P_1 becomes equal to 0.17.

When L is reduced to 10 μm and $\Delta = +60$ MHz, the value of P_3 decreases further to 0.0002, P_2 decreases to 0.06, and P_1 is saturated with a value of 0.2 (Fig. 4g). At $\Delta = 0$ (Fig. 4h) for this L a complete blockade is achieved: P_3 decreases to 0.0001, P_2 decreases to 0.005, and P_1 remains equal to 0.17.

To increase the value of P_1 in the case of a full dipole blockade in the three-atom mode, it is necessary to reduce the Rabi frequency by a factor of $\sqrt{3}$ to 0.14 MHz. Such spectra are presented in Figs 4i and 4j for $L = 10$ μm. Now, with $\Delta = +60$ MHz, the value of P_3 remains at the level of 0.0002, P_2 is 0.04, and P_1 increases to 0.967 (Fig. 4i). When $\Delta = 0$ (Fig. 4j), complete blockade is achieved: $P_3 = 0.00005$, $P_2 = 0.002$ and $P_1 = 0.998$. Thus, in the case of three disordered atoms, which represent the 'Rydberg superatom' [8, 21, 22], the fidelity of quantum gates based on dipole blockade up to 99.8% can also be achieved, and the presence of a nonzero energy defect for the Förster resonance impairs the fidelity by an order of magnitude.

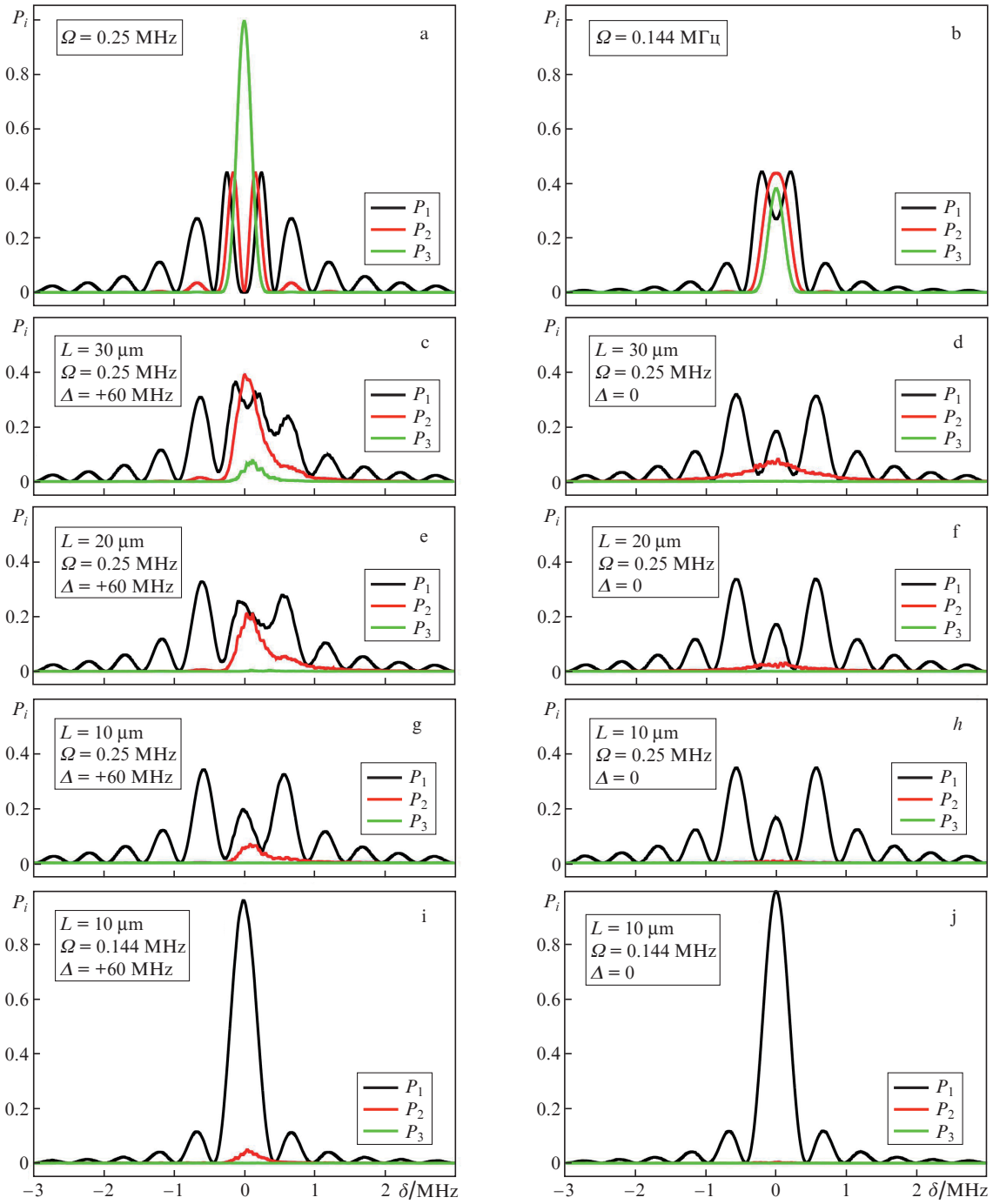

Figure 4. (Colour online) Calculated probability spectra of the single-atom (P_1), two-atom (P_2), and three-atom (P_3) excitation of the Rydberg state $120P_{3/2}$ by a square laser pulse having the duration 2 μs with different Rabi frequencies Ω for (a, b) three noninteracting and (c–j) interacting Rb atoms randomly positioned in the cubic volume of laser excitation with a linear size L, for various detunings from the Förster resonance Δ and the width of the laser line $\Gamma = 0$.

5. Effect of line width on the accuracy of the dipole blockade

All the results of theoretical calculations, shown in Figs 3 and 4, represent an idealised picture that does not take into account the many factors arising in the experimental implementation. The main one is the nonmonochromaticity of laser radiation, due to the finite width of the exciting radiation line. The presence of fluctuations in the frequency of laser radiation can lead to blurring and a decrease in the contrast of Rabi oscillations [13]. Accordingly, even with a strong interaction of Rydberg atoms, the maximum achievable accuracy of the dipole blockade will also decrease.

As an example, Fig. 5 shows the same spectra of single-atom and two-atom laser excitation as in Fig. 3, but with the introduction of laser radiation frequency fluctuations having a Gaussian distribution with a half-maximum width $\Gamma = 1$ MHz into a theoretical model. In contrast to Fig. 3, the spectra are averaged not only by 1000 random positions of two atoms in the excitation volume, but also by 1000 random values of the

frequency within the width of the line. As a result, in Fig. 5 one can see the complete disappearance of the Rabi oscillations, although the effect of the dipole blockade is preserved. Now at Δ = +60 MHz, the minimum value of P_2 is 0.004, however, the value of P_1 is only 0.32 (Fig. 5i). When $\Delta = 0$, we have $P_2 = 0.0004$ and $P_1 = 0.33$ (Fig. 5j). This is a consequence of the fact that for such a line width the incoherent excitation of collective states is realised [13, 19], in which the probability of single-atom excitation under the conditions of a dipole blockade never reaches 1 and it is almost impossible to perform quantum gates with high fidelity. The situation can be somewhat improved by an increase in the Rabi frequency, but under the incoherent excitation the probability of P_1 will still reach saturation and will not exceed 0.5.

In this connection, a natural question arises about the line width acceptable for performing quantum gates on the basis of a dipole blockade in Rydberg atoms. For example, our theoretical calculations for Γ = 0.1 MHz showed that the spectra obtained visually practically do not differ from the spectra in Figs 3i and 3j, and the contrast of Rabi oscillations decreases insignificantly. However, for Δ = +60 MHz, we obtain $P_2 = 0.014$ and $P_1 = 0.95$, and for $\Delta = 0$, we have $P_2 = 0.001$ and $P_1 = 0.96$. Thus, compared with Fig. 3, the values of P_2 remained almost unchanged, but the values of P_1 decreased by 4%–5%. The fidelity of quantum gates will also decrease. This fidelity is unacceptable, since the quantum computing with error correction requires the fidelity of individual quantum gates above 99% [12].

As a result of the extended numerical simulation, we found the dependences on the line width Γ for the probabilities of the single-atom (P_1) and two-atom (P_2) excitation of the Rydberg state $120P_{3/2}$ by a rectangular laser pulse with a duration of 2 μs, the Rabi frequency Ω = 0.177 MHz at L equal to 10 or 20 μm and the detuning from the Förster resonance Δ equal to 0 or +60 MHz (Fig. 6). The worst situation is observed for L = 20 μm and Δ = +60 MHz: even at a zero

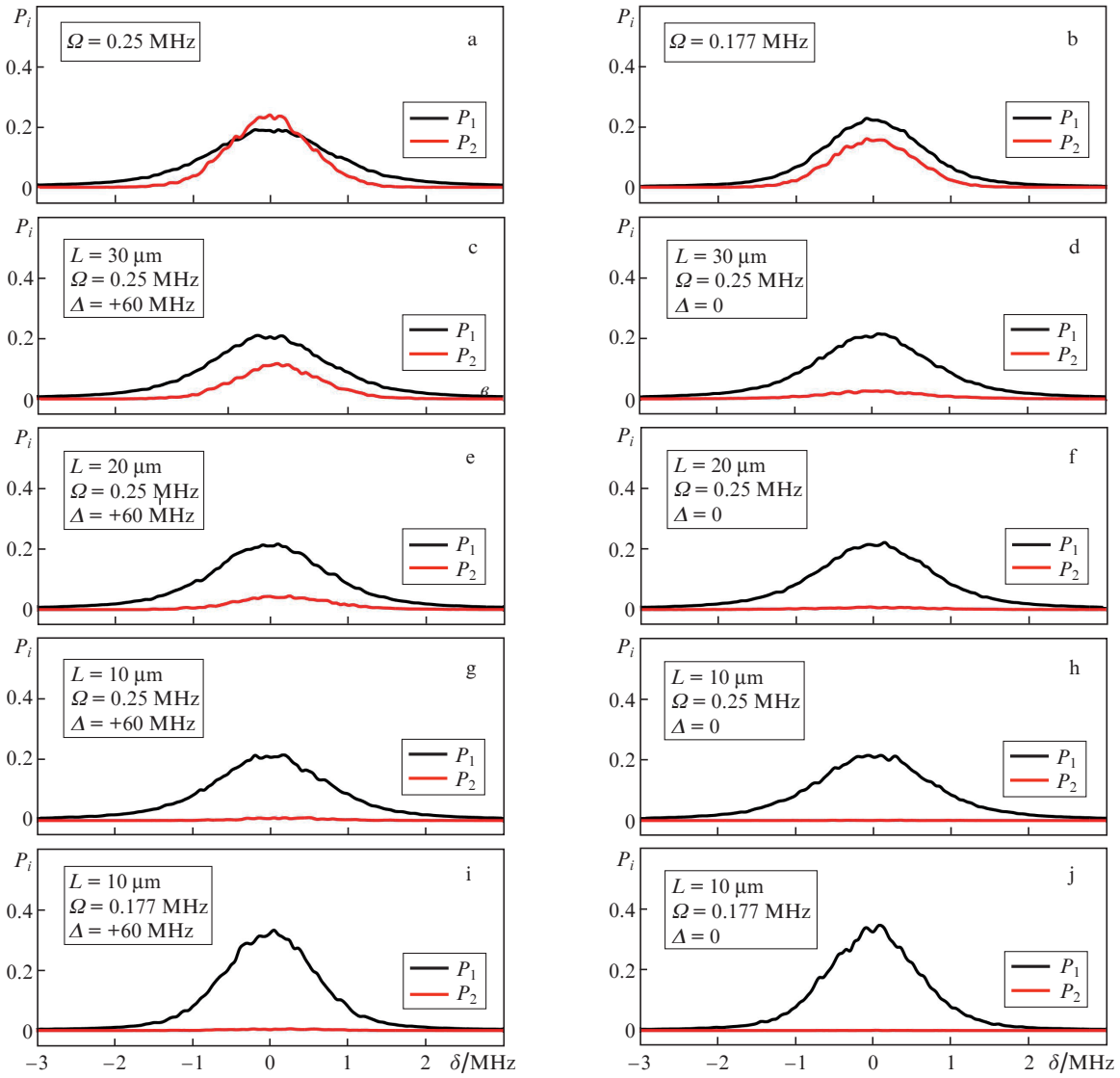

Figure 5. (Colour online) Calculated probability spectra of the single-atom (P_1) and two-atom (P_2) excitation of the Rydberg state $120P_{3/2}$ by a rectangular laser pulse having the duration 2 μs with different Rabi frequencies Ω for (a, b) two noninteracting and (c–j) interacting Rb atoms randomly positioned in the cubic volume of laser excitation with a linear size L, for various detunings Δ from the Förster resonance and the width of the laser radiation line Γ = 1 MHz.

line width, the probability P_1 does not exceed 0.92, and P_2 is at the level of 0.1. For the same Δ, at $L = 10$ μm, the situation improves: $P_1 \approx 0.97$, and $P_2 \approx 0.02$. The best results are obtained for $\Delta = 0$: at $L = 20$ μm the probability P_1 increases to 0.98, and P_2 decreases to 0.01, at $L = 10$ μm, we have $P_1 = 0.999$ and $P_2 = 0.001$.

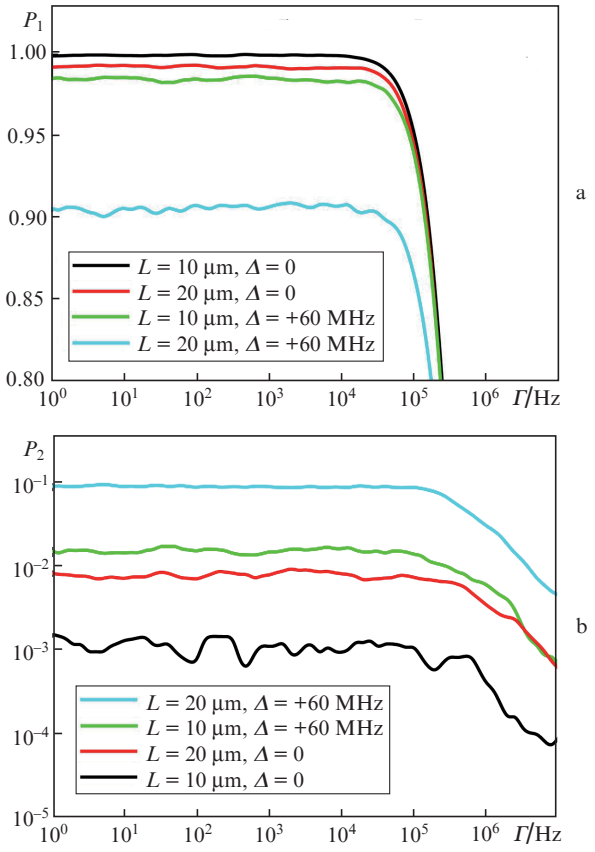

Figure 6. (Colour online) Calculated dependences on the line width Γ of the probabilities of the (a) single-atom and (b) two-atom excitation of the Rydberg state $120P_{3/2}$ by a rectangular laser pulse having the duration 2 μs with a Rabi frequency of $\Omega = 0.177$ MHz for two Rb atoms randomly positioned in the cubic volume of the laser excitation.

The dependences in Fig. 6 have a threshold character, and the thresholds are noticeably different for P_1 and P_2 for the used laser pulse parameters. The value of P_1 begins to decrease at a line width exceeding 10–20 kHz, while for P_2 the threshold occurs at 100 kHz. This suggests that P_1 is most sensitive to the line width, which should be guided by when assessing the accuracy of quantum gates based on dipole blockade. Thus, for the conditions considered, the limiting line width should not exceed 10 kHz, which requires special measures to stabilise the frequency of most modern solid-state tunable lasers that have a line width of about 0.1–1 MHz in free-running mode. Similar conclusions based on the experiments were presented in a number of papers by other authors [23–26].

A general conclusion can be made that to achieve high accuracy of the dipole blockade, the condition $\Gamma/(2\pi) \ll 1/\tau$ must be met, i.e., the technical line width must be much smaller than the Fourier width of the laser pulse spectrum. Therefore, if in experiments it is not possible to reduce the width of the laser line, one may use shorter laser pulses, while increasing the Rabi frequency. However, in this case it may become necessary to have a stronger interaction of Rydberg atoms by reducing the average distance between them.

6. Conclusions

In the present work, the effect of the dipole blockade on the laser excitation spectra of mesoscopic ensembles of Rydberg atoms is theoretically investigated. In most other papers on this topic, the features of changes in the laser excitation spectra under complete or partial dipole blockade were not discussed. At the same time, they may carry additional information about the degree of blockade and the influence of various factors on it. According to the results of the research we can draw the following conclusions.

First, Rydberg atoms experience either resonance dipole–dipole interaction or nonresonance van der Waals interaction. The transition from one type of interaction to another can be described by means of Förster resonances driven by an electric field. We considered an example of such a resonance for the high Rydberg state $120P_{3/2}$ in Rb atoms. It was found that the defect in the energy of this resonance (+60 MHz in the absence of an electric field) significantly affects the fidelity of the dipole blockade, reducing it by about an order of magnitude. Therefore, despite the technical complexity of using control electric fields in experiments with ultracold atoms, to increase fidelity, it is recommended to use only resonant dipole–dipole interaction of Rydberg atoms with a zero defect in the energy of the Förster resonance, which is achieved by applying a combination of dc and radio-frequency electric fields.

Second, an increase in the number of atoms in the mesoscopic ensemble leads to a significant change in the spectra compared with the spectra for two atoms. Nevertheless, we have shown that even in the case of three atoms in an ensemble, it is possible to achieve the full dipole blockade mode with resonance dipole–dipole interaction, although with some decrease in its fidelity. This allows implementation of various quantum computing schemes for the so-called superatoms, in which qubits are represented not by single atoms, but by mesoscopic atomic ensembles.

Third, the fidelity of the dipole blockade strongly depends on the line width of exciting laser radiation. Despite the fact that the blockade effect itself is preserved, with an increase in the width of the line, the Rabi oscillations blur and the probability of laser excitation decreases significantly. In this case, the dependence of the accuracy on the line width has a threshold character. We have shown that for laser pulses with a duration of 2 μs, it is necessary to have a line width of less than 10 kHz, which requires special measures to stabilise the radiation frequency of most lasers.

Acknowledgements. The work was supported by the Russian Foundation for Basic Research [Grant Nos 19-52-15001 (with regard to the analysis of Förster resonances) and 17-02-00987 (with regard to the applications in quantum information)], by the Russian Science Foundation [Grant No. 18-12-00313 (with regard to the dipole blockade analysis)], and by Novosibirsk State University.

References

1. Gallagher T.F. *Rydberg Atoms* (Cambridge: Cambridge University Press, 1994).

2. Saffman M., Walker T.G., Mølmer K. *Rev. Mod. Phys*., **82**, 2313 (2010).
3. Ryabtsev I.I., Beterov I.I., Tret'yakov D.B., Entin V.M., Yakshina E.A. *Phys. Usp.*, **59**, 196 (2016) [*Usp. Fiz. Nauk*, **182**, 206 (2016)].
4. Jaksh D., Cirac J.I., Zoller P., Rolston S.L., Cote R., Lukin M.D. *Phys. Rev. Lett*., **85**, 2208 (2000).
5. Beterov I.I., Saffman M., Yakshina E.A., Tretyakov D.B., Entin V.M., Bergamini S., et al. *Phys. Rev. A*, **94**, 062307 (2016).
6. Beterov I.I., Hamzina G.N., Yakshina E.A., Tretyakov D.B., Entin V.M., Ryabtsev I.I. *Phys. Rev. A*, **97**, 032701 (2018).
7. Beterov I.I., Khamzina G.N., Tret'yakov D.B., Entin V.M., Yakshina E.A., Ryabtsev I.I. *Quantum Electron*., **48** (5), 453 (2018) [*Kvantovaya Elektron*., **48** (5), 453 (2018)].
8. Lukin M.D., Fleischhauer M., Cote R., Duan L.M., Jaksch D., Cirac J.I., Zoller P. *Phys. Rev. Lett*., **87**, 037901 (2001).
9. Isenhower L., Urban E., Zhang X.L., Gill A.T., Henage T., Johnson T.A., Walker T.G., Saffman M. *Phys. Rev. Lett*., **104**, 010503 (2010).
10. Wilk T., Gaetan A., Evellin C., Wolters J., Miroshnichenko Y., Grangier P., Browayes A. *Phys. Rev. Lett*., **104**, 010502 (2010).
11. Comparat D., Pillet P. *J. Opt. Soc. Am. B*, **27**, A208 (2010).
12. Saffman M. *J. Phys. B*, **49**, 202001 (2016).
13. Yakshina E.A., Tret'yakov D.B., Entin V.M., Beterov I.I., Ryabtsev I.I. *Quantum Electron*., **48** (10), 886 (2018) [*Kvantovaya Elektron*., **48** (10), 886 (2018)].
14. Ryabtsev I.I., Tretyakov D.B., Beterov I.I., Entin V.M., Yakshina E.A. *Phys. Rev. A*, **82**, 053409 (2010).
15. Yakshina E.A., Tretyakov D.B., Beterov I.I., Entin V.M., Andreeva C., Cinins A., Markovski A., Iftikhar Z., Ekers A., Ryabtsev I.I. *Phys. Rev. A*, **94**, 043417 (2016).
16. Tretyakov D.B., Entin V.M., Yakshina E.A., Beterov I.I., Andreeva C., Ryabtsev I.I. *Phys. Rev. A*, **90**, 041403(R) (2014).
17. Kamenski A.A., Manakov N.L., Mokhnenko S.N., Ovsiannikov V.D. *Phys. Rev. A*, **96**, 032716 (2017).
18. Beterov I.I., Ryabtsev I.I., Tretyakov D.B., Entin V.M. *Phys. Rev. A*, **79**, 052504 (2009).
19. Entin V.M., Yakshina E.A., Tretyakov D.B., Beterov I.I., Ryabtsev I.I. *JETP*, **116**, 721 (2013) [*Zh. Eksp. Teor. Fiz*., **143** (5), 831 (2013)].
20. Kamenski A.A., Ovsiannikov V.D. *J. Phys. B*, **47**, 095002 (2014).
21. Stanojevic J., Côté R. *Phys. Rev. A*, **80**, 033418 (2009).
22. Beterov I.I., Saffman M., Yakshina E.A., Tretyakov D.B., Entin V.M., Hamzina G.N., Ryabtsev I.I. *J. Phys. B*, **49**, 114007 (2016).
23. Levine H., Keesling A., Omran A., Bernien H., Schwartz S., Zibrov A.S., Endres M., Greiner M., Vuletić V., Lukin M.D. *Phys. Rev. Lett*., **121**, 123603 (2018).
24. Léséleuc S., Barredo D., Lienhard V., Browaeys A., Lahaye T. *Phys. Rev. A*, **97**, 053803 (2018).
25. Sautenkov V.A., Saakyan S.A., Bobrov A.A., Vilshanskaya E.V., Zelener B.B., Zelener B.V. *J. Opt. Soc. Am. B*, **35**, 1546 (2018).
26. Saakyan S.A., Sautenkov V.A., Zelener B.B. *J. Phys.: Conf. Ser*., **946**, 012128 (2018).